ANTICANCER RESEARCH *43*: 1437-1448 (2023)
doi:10.21873/anticanres.16292

Expression of Eukaryotic Translation Initiation Factors in the Urothelial Carcinoma of the Bladder

JETON LUZHA[1], NORBERT NASS[2], PIOTR CZAPIEWSKI[3], NICOLAS SCHROEDER[4], THOMAS KALINSKI[5], MARTIN SCHOSTAK[6], CHRISTOPH SCHATZ[7], BURKHARD JANDRIG[6] and JOHANNES HAYBAECK[7,8]

[1]*Department of Otorhinolaryngology, Head and Neck Surgery, Friedrich-Alexander-University Erlangen-Nürnberg (FAU), Erlangen, Germany;*
[2]*Dessau Medical Center and Brandenburg Medical School Theodor Fontane, Dessau-Roßlau, Germany;*
[3]*Institute of Pathology, Municipal Clinic Dessau, Dessau-Roßlau, Germany;*
[4]*Joint Practice for Pathology, Berlin, Germany;*
[5]*Joint Practice for Pathology, Hamburg, Germany;*
[6]*Department of Urology and Pediatric Urology, Otto-von-Guericke-University, Magdeburg, Germany;*
[7]*Institute of Pathology, Neuropathology and Molecular Pathology, Medical University of Innsbruck, Innsbruck, Austria;*
[8]*Diagnostic & Research Center for Molecular BioMedicine, Institute of Pathology, Medical University of Graz, Graz, Austria*

Abstract. *Background/Aim: Urothelial carcinoma (UC) of the urinary bladder is the second most common tumor in the field of urology and is characterized by a relatively aggressive growth behavior. New therapeutic approaches are required to improve the prognosis of affected patients. We hypothesized a link between dysregulation of eIFs and the development of UC. Therefore, in the present work, we investigated the expression behavior of eIF1, eIF1AY, eIF1AX, eIF2α, eIF3a, eIF3b, eIF4B, eIF4E, eIF4G, eIF5A, eIF5B, and eIF6 in UC compared with that in urothelial tissue. Materials and Methods: Paraffin-embedded tumor tissue samples from 107 patients suffering from UC were examined. Seventy-six patients contained adjacent urothelial tissue. Three tumor tissue cylinders (tumor collective) and two urothelial tissue cylinders (control collective) were collected per patient and embedded in tissue microarray (TMA) blocks. Immunohistochemical staining of the TMA sections was then performed. The staining results were assessed semi-quantitatively. Staining intensities and immunoreactive scores (IRS) of both collectives were compared. In each case, a distinction was made between cytoplasmic and nuclear staining. Results: Significant up-regulation of eIF1AY, eIF2α, eIF3a, eIF3b, eIF4B, eIF4G, eIF5B, and eIF6 was found in the cytoplasm of UC. In contrast, eIF1 and eIF5A were significantly down-regulated in the cytoplasm of UC. eIF5A and eIF6 were significantly down-regulated in the nuclei of UC. Conclusion: Dysregulation of eIFs in the urothelium of the urinary bladder is linked to carcinogenesis at this site.*

Correspondence to: Johannes Haybaeck, Institute of Pathology, Neuropathology and Molecular Pathology, Medical University of Innsbruck, 6020 Innsbruck, Austria. Tel: +43 512900371300, e-mail: johannes.haybaeck@i-med.ac.at

Key Words: Translation, initiation, eukaryotic initiation factors (eIFs), bladder cancer, urothelial carcinoma.

The urothelial carcinoma (UC) of the urinary bladder accounts for the second most common tumor in the subject area of urology and is characterized by a relatively aggressive growth behavior. According to the Center for Cancer Registry Data at the Robert Koch Institute, approximately 22,400 men and 7,100 women in Germany developed UC (Ta, Tis, T1-T4) in 2014. In the presence of metastases, the 10-year survival rate drops well below 10%. Numerous risk factors responsible for the development of UC have been demonstrated. The main undisputed risk factor is smoking (1-3). Tobacco contains numerous carcinogenic substances such as nitrosamines, which have been linked to the development of UC (4). Occupational exposure to carcinogenic substances has been confirmed as a risk factor as well as working exposures in the dye and metal industries and hairdressing profession, could be associated with the development of UC (1, 3, 4). Male sex, chronic inflammation of the urinary bladder, arsenic-containing drinking water, radioactive radiation, and cyclophosphamide are also considered to be risk factors for UC (1, 3-5).

In the process of translation, a cell translates the genetic information of the messenger ribonucleic acid (mRNA) into a corresponding polypeptide. Translation is tightly regulated and divided into four main steps: Initiation, elongation, termination, and ribosomal recycling.

There are several mechanisms of eukaryotic translation. The canonical, cap-dependent translation represents the main mechanism. In addition, a cap-independent mechanism also exists, which is facilitated by internal ribosome entry sites (IRES) (6, 7).

The main players of eukaryotic translation initiation are the eukaryotic initiation factors (eIFs) consisting of eIF1, eIF1A, eIF2, eIF2B, eIF3, eIF4A, eIF4E, eIF4G, eIF4B, eIF4H, eIF5, eIF5B and eIF6. Translation of mRNA occurs at ribosomal subunits (UE) 40S and 60S. In this process, the eIFs enable and coordinate the ideal course of initiation. Dysregulation of eIFs can lead to tumor growth (7-9). Aberrant translation can result in preferential translation of oncogenic mRNA sequences that tumors require to maintain malignant growth processes (10).

The cap-dependent pathway of translation initiation can be simplified into four main steps and begins with the formation of the 43S preinitiation complex (PIC). This is composed of eIF1, eIF1A, eIF3, eIF5, the ribosomal 40S-UE, and the methionine-transfer RNA-eIF2-GTP complex (Met-tRNA-eIF2-GTP complex), also known as the ternary complex (TC).

This is followed by the formation of the 48S-PIC. For this, the mRNA is recruited to the 43S-PIC with the help of the eIF4F complex. eIF4F is a heterotrimeric complex composed of eIF4A, eIF4E and eIF4G. The eIF4F complex and eIF4B recognize and bind to the 5' cap of mRNA. The mRNA-eIF4F complex then binds to the 43S PIC. The mRNA is then scanned in a 5'-3' direction until a corresponding adenine-uracil-guanine (AUG) start codon is found. The latter step is facilitated by eIF1 and eIF1A. After successful attachment of the anti-codon sequence of the Met-tRNA-eIF2-GTP complex to the start codon of the mRNA, guanosine triphosphate (GTP) is hydrolyzed and eIF2-guanosine diphosphate (GDP), eIF1, eIF3, and eIF5 are released. Subsequently, the 60S-UE binds to the 48S initiation complex with the help of eIF5B and eIF6. After correct binding, eIF5B is hydrolyzed and dissociates to form a translatable 80S complex. Subsequently, eIF1A also dissociates from the complex (7-9, 11-15). As the pace-keeping mechanism of the protein biosynthesis, the eIFs play a major part in the initial step. In case of dysregulation of protein biosynthesis as seen in cancer, eIFs may function as therapeutic targets. The aim of the study was to identify eIFs that may potentially function as therapeutic targets and prognostic biomarkers.

Materials and Methods

Data collection of the patient collective. This study included 107 patients who were treated for their UC disease by transurethral resection of the urinary bladder (TUR-B) or cystectomy at the Department of Urology, University Hospital Magdeburg, Germany, between 2010 and 2018. Corresponding paraffine blocks with tumor tissue were selected from the archives of the Institute of Pathology at Magdeburg University Hospital and tested for suitability for the production of tissue microarrays (TMAs). Informed consent was obtained from all subjects involved in the study. The study was performed with review and approval of the Ethics Committee of the University of Magdeburg (ethics vote number 21/19). Clinical-pathological patient data were stored in a Microsoft Excel 2016 database. The following patient data were collected:

Last name, first name, date of birth, sex, case number, time of initial diagnosis, histo-pathological diagnosis of the tumor, T stage, and tumor differentiation grade. In the further course, the data were used pseudonymously.

Among the 107 patients with UC (tumor collective), 76 patients also showed adjacent non-neoplastic altered urothelium (control group). 16.8% of patients (n=18) were female with an average age of 73 years. Men were represented with 83.2% (n=89) with an average age of 71 years. The ratio between men and women was nearly 5:1. The average age was 71 years with a median of 73 years. The youngest patient was 46, and the oldest was 91 years old based on the date of the first diagnosis.

Low-grade UC comprised 8.4% (n=9) of cases and high-grade carcinomas comprised 87.9% (n=94). No grading was possible in 3.7% of patients (n=4). The tumor T stages were as follows:

Ta: 0.9% (n=1), T1: 5.6% (n=6), T2: 47.7% (n=51), T3: 30.8% (n=33), T4: 15.0% (n=16).

Archive and selection criteria. The data of the formalin fixed paraffin-embedded (FFPE) tissue samples were collected from the laboratory information system ISP (Imassense, Berlin, Germany) of the University Hospital Magdeburg. Blocks were selected for sufficient tumor material for the creation of TMAs. Non-neoplastic urothelial tissue was included. For each tumor block, Hematoxylin-Eosin (HE) stained slides were obtained and were additionally investigated for suitability for the study by two independent and board-certified pathologists (TK, NS). Vital, non-necrotic tumor tissue, and urothelial non-neoplastic tissue (NNT) were marked according to the positions on the slides. According to the marked area on the slide, tissue cylinders were punched out from the corresponding FFPE tissue. Considering the clinicopathological parameters, 107 cases were suitable for the creation of TMAs by the Tissue Arrayer MTA-Booster (Version 01), (Alphelys, Plaisir, France). In total, 76 patients out of 107 also harbored healthy urothelial NNT.

Generation of TMAs. The creation of TMAs was executed with a Manual-Tissue-Arraying instrument (MTA Booster, Version 01, Alphelys, France).

To avoid random staining events, three tumor tissue cylinders and two urothelial cylinders as control were obtained. For obtaining tumor tissues, hollow needles with a diameter of 0.6 mm were used. To ensure that urothelial tissue was obtained, hollow needles with a diameter of 1.0 mm were used. A total of nine TMAs were created. The TMAs were placed in an incubator at 40°C to embed the tissue cylinders into paraffin. A motorized Zeiss Hyrax M55 rotation microtome (Zeiss, Oberkochen, Germany) was used for cutting 4 μm thick slices. After smoothing in a water bath, slices were fixed onto Polysine adhesion slides (Thermo Scientific, Waltham, MA, USA). Eleven slices were prepared on 9 TMAs to be probed with antibodies against 11 eIFs.

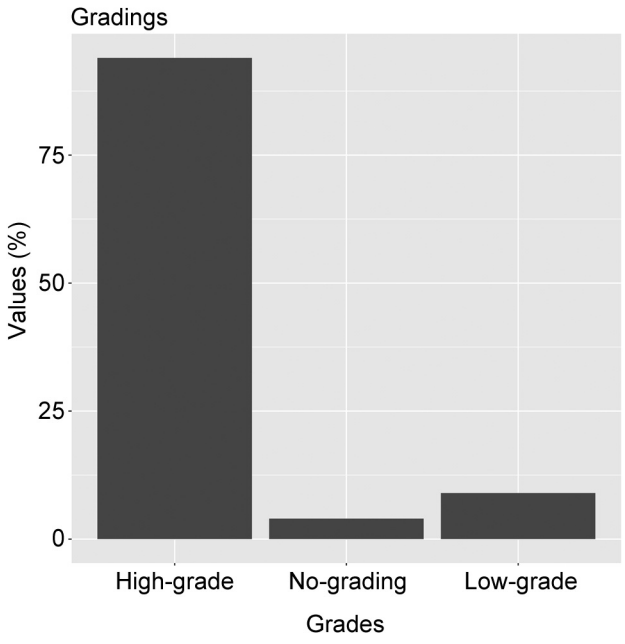

Figure 1. *Number of patients according to grade.*

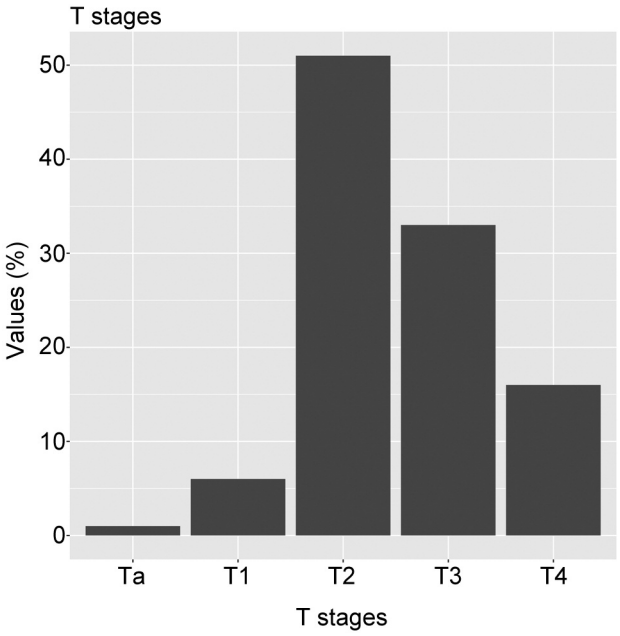

Figure 2. *Number of patients according to T stages.*

Table I. *Primary antibodies used for detection.*

Antibody	Producer	Order number	Dilution	Method
eIF1, monoclonal	Thermo Fisher, Waltham, MA, USA	MA1-077	1:3,000 CC1 mild	DAB Benchmark Ultra
eIF1AY	Thermo Fisher (Invitrogen), Waltham, MA, USA	PA5-31198	1:500 CC1 mild	DAB Benchmark Ultra
eIF2α (D7D3) XP	Cell Signalling, Danvers, MA, USA	#5324P	1:2,000 CC1 mild	DAB Benchmark Ultra
eIF3a	Thermo Fisher (Invitrogen), Waltham, MA, USA	PA5-31296	1:50 CC1 mild	DAB Benchmark Ultra
eIF3B (eIF3η D-9)	Santa Cruz, Dellas, TX, USA	Sc-137215	1:50 CC1 mild	DAB Benchmark Ultra
eIF4b	GeneTex, Alton Pkwy Irvine, CA, USA	GTX33175	1:500 CC1 mild	DAB Benchmark Ultra
eIF4e	Cell Signalling, Danvers, MA, USA	#9742	1:100 CC1 mild	DAB Benchmark Ultra
eIF4g	Cell Signalling, Danvers, MA, USA	#2498	1:50 CC1 mild	DAB Benchmark Ultra
eIF5a	Thermo Fisher (Invitrogen), Waltham, MA, USA	PA5-29204	1:250 CC1 mild	DAB Benchmark Ultra
eIF5b	Thermo Fisher (Invitrogen), Waltham, MA, USA	PA5-36456	1:50 CC1 mild	DAB Benchmark Ultra
eIF6	Biomol/BETHYL, Hamburg, Germany	A303030A/M	1:100 CC1 mild	DAB Benchmark Ultra

Patient collective. For the study, tumor tissue samples from 107 patients with UC were examined immunohistochemically (tumor collective). Of these 107 patient samples, 76 contained urothelial NNT and were suitable as a control collective for the expression analyses. Figure 1 shows the distribution of the grades among the patients' collective, and Figure 2 shows the distribution of the T stages in the patient cohort.

Immunohistochemistry (IHC)

The TMAs were stained for eIF1, eIF1aY, eIF2α, eIF3a, eIF3b, eIF4b, eIF4e, eIF4g, eIF5a, eIF5b, and eIF6 (Table I) using the BenchMark Ultra stainer (Ventana Medical Systems, Tucson, AZ, USA). For demasking, the antigen Cell Conditioning Solution (CC1-mild, Ventana Medical Systems) was added. Primary antibody incubation time was 32 min. To detect the reaction, the ultraVIEW Universal DAB Detection Kit (Ventana) was used. The detection included the HRP masked secondary antibodies (horseradish peroxidase) as well as 3,3'-diaminobenzidin-tetrahydrochloride chromogen leading to a brown precipitate. A core counter staining was achieved with Hematoxylin according to Mayer. Dehydration was performed with Xylol and ethyl alcohol. Canada balm was used for covering the slides.

Evaluation of the immunohistochemical staining. The 99 slides were scanned using a NanoZoomer 360S Whole Slide Imaging Scanner from Hamamatsu (Hamamatsu City, Japan). The images were evaluated semi-quantitatively with the use of the program NanoZoomer-Digital-Pathology (NDP.View2) by PC and JL. Default options were chosen for evaluation.

Each TMA spot was evaluated separately. If two or three spots were available, the median score of the replicates per patient was built. If only one sample per patient was available, the score for the sample was calculated. Spots of poor optical quality such as fragmented and debris samples on the TMA were not evaluated. The staining intensity of 5-200 spots (I, Intensity from 0 to 3) and the percentual part of the stained tumor area (D, Density from 0 to 100%) were determined and the median was calculated for I and for D. Spots were differentiated into cytoplasmic, nuclear, or cytoplasmic-nuclear staining. The ordinal values for the intensity staining were (0 – negative staining reaction, 1 – weak positive staining reaction, 2 – moderate strong positive staining reaction, 3 – strong positive staining reaction). The median was calculated and was multiplied by the percentual part of the stained area. The product was divided by 10 to retrieve an immunoreaction score (IRS score from 0 to 30) per patient. Equation 1 was used:

$$IRS = \frac{I \cdot D}{10} \quad (1)$$

Statistical evaluation. The data were evaluated with IBM SPSS Statistics Version 22, (Armonk, NY, USA).

For each eIF, descriptive statistics such as mean, median, standard deviation, and interquartile range were used in order to calculate the average cytoplasmic and nuclear staining intensity and for the average IRS.

To compare the staining intensities between tumor and control samples, the non-parametric, unpaired Wilcoxon–Mann–Whitney–*U* signed-rank test was used. A *p*-value below 0.05 was considered significant.

Results

Expression of eIF1. For eIF1, staining was evaluable in 103 patients of the tumor collective and 73 of the NNT collective. eIF1 was very weakly expressed in both tumor and NNT tissue. On average, stronger e staining was found in the cytoplasm compared to the nucleus. The average cytoplasmic staining in the UC was 0.23 (IRS=1.81). No staining was observed in 80 out of 103 cases (77.7%), a weak staining was obtained in 22 of 103 cases (21.4%) and in only one case (1.0%) a moderately strong staining was retrieved. The NNT on the other hand, exhibited a significantly higher staining with an average cytoplasmic staining intensity of 0.75 (IRS=6.80) combined with a significantly higher staining for eIF1 (p=0.000). Predominantly weak staining (36 of 73 cases, 49.3%) was found. In 25 of 73 cases (34.2%) no staining was observed and in only 12 cases (16.4 %) a moderately strong staining was detectable. The tumor and NT collectives showed on average a similar nuclear expression of eIF1 (Table II, Figure 3, Figure 4).

Expression of eIF1aY/elF1aX. Next to eIF2α and eIF6, EIF1aY exhibited the strongest staining in UC. A total of 105 stainings of the tumor collective and 74 of the NNT collective were included in the statistical analysis. EIF1aY was exclusively detected in the cytoplasm and expressed in the nucleus (CN) in only one case of the tumor collective. EIF1aY showed strong cytoplasmic staining in UC (I=2.76, IRS=26.92) in 85 of 105 tumor samples (81.0%). Seventeen cases (16.2%) showed moderately strong staining. Only 1 case (1.0 %) revealed weak cytoplasmic staining. In 2 cases (1.9%), no staining was detected. In healthy urothelial NNT, on the other hand, the average cytoplasmic staining intensity was only 1.16

Table II. *Analyzed translation factors, the location, type, number of samples, average staining intensity, average IRS, and p-value*.

eIF	Localization	Type	n	Ø Staining intensity	Ø IRS	*p*-Value
eIF1	Cytosol	Tumor	103	0.23	1.81	0.000
		NNT	73	0.75	6.80	
	Nucleus	Tumor	103	0.18	0.23	0.554
		NNT	73	0.17	1.33	
eIF1aY	Cytosol	Tumor	105	2.76	26.92	0.000
		NNT	74	1.16	10.32	
	Nucleus	Tumor	105	0.03	0.00	0.317
		NNT	74	0.00	0.00	
eIF2α	Cytosol	Tumor	105	2.74	27.43	0.000
		NNT	74	1.94	19.13	
	Nucleus	Tumor	105	0.06	0.40	0.157
		NNT	74	0.00	0.00	
eIF3a	Cytosol	Tumor	103	1.57	15.55	0.002
		NNT	76	1.21	12.11	
	Nucleus	Tumor	103	0.03	0.14	0.180
		NNT	76	0.00	0.00	
eIF3b	Cytosol	Tumor	105	1.92	18.68	0.000
		NNT	74	1.07	10.25	
	Nucleus	Tumor	105	0.00	0.00	1.000
		NNT	74	0.00	0.00	
eIF4b	Cytosol	Tumor	105	1.56	15.60	0.000
		NNT	75	1.09	10.76	
	Nucleus	Tumor	105	0.10	0.72	0.125
		NNT	75	0.04	0.33	
eIF4e	Cytosol	Tumor	104	1.66	16.59	0.431
		NNT	72	1.52	15.16	
	Nucleus	Tumor	104	0.01	0.05	0.317
		NNT	72	0.00	0.00	
eIF4G	Cytosol	Tumor	105	2.27	22.67	0.000
		NNT	73	1.56	15.36	
	Nucleus	Tumor	105	0.00	0.00	1.000
		NNT	73	0.00	0.00	
eIF5a	Cytosol	Tumor	105	1.19	11.81	0.005
		NNT	72	1.48	14.33	
	Nucleus	Tumor	105	0.06	0.29	0.001
		NNT	72	0.38	2.09	
eIF5b	Cytosol	Tumor	105	1.81	17.22	0.000
		NNT	74	1.25	11.05	
	Nucleus	Tumor	105	0.02	0.08	0.655
		NNT	74	0.01	0.01	
eIF6	Cytosol	Tumor	104	2.56	25.35	0.000
		NNT	74	1.72	16.64	
	Nucleus	Tumor	104	0.97	4.62	0.040
		NNT	74	1.24	7.20	

Ø: Average.

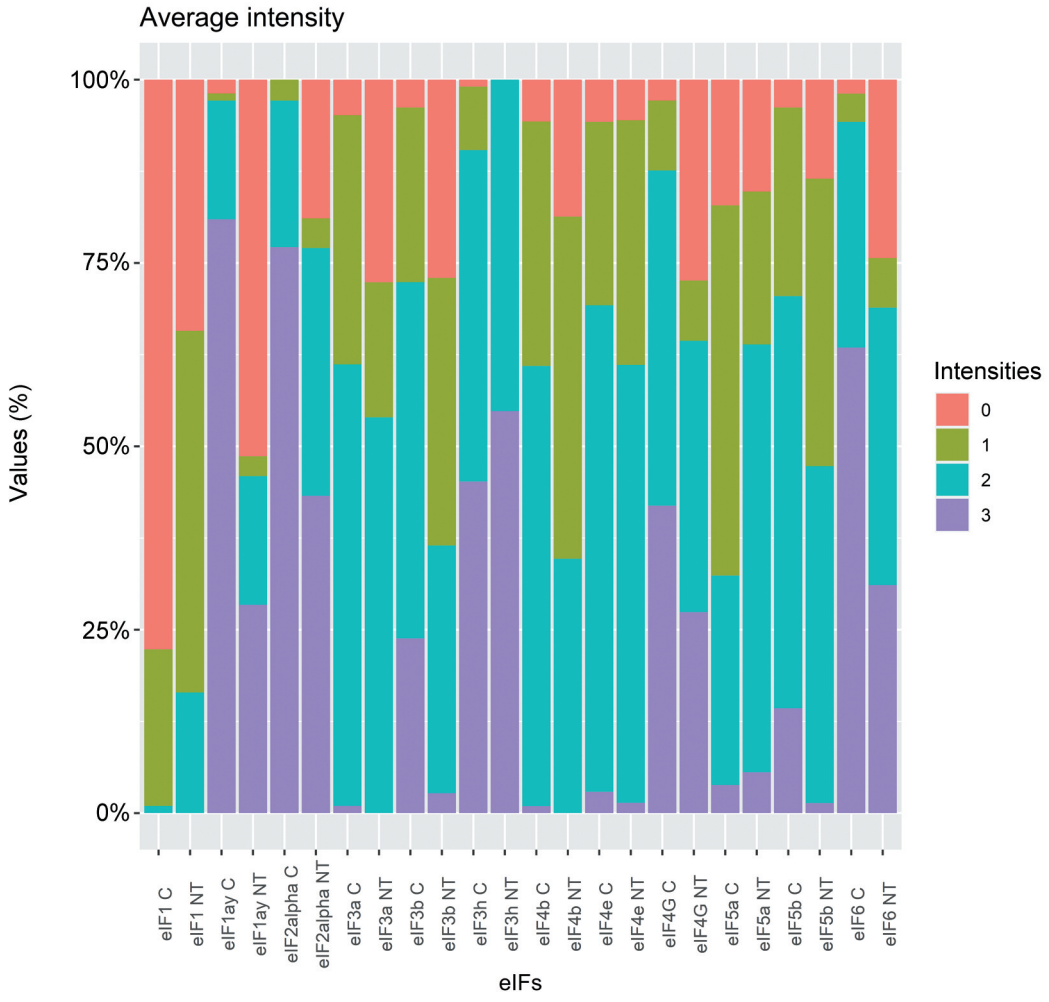

Figure 3. *The percentage of each eIF intensity score per cancer (C) and non-neoplastic tissue (NNT) across all samples.*

(IRS=10.32) and was undetectable in most cases (38 of 74 cases, 51.4%). Interestingly, in 21 out of 74 cases (28.4%) a strong staining was observed. The U-test resulted on average in a significantly higher cytoplasmic staining intensity of eIF1aY in the UC (p>0.000) (Table II, Figure 3, Figure 4).

Expression of eIF2α. For eIF2α staining, 105 patients of the tumor collective and 74 cases of the NNT collective were analyzed. eIF2α showed strong cytoplasmic staining of 2.74 (IRS=27.43) in the UC. There was strong staining in 81 of 105 cases (77.1%), a medium staining in 21 (20.0%), and a weak staining in 3 (2.9%) cases. In the cytoplasm of the NNT collective, eIF2α showed moderate staining intensity with an average of 1.94 (IRS=19.13). EIF2α was significantly up-regulated in the cytoplasm of UC cells (p>0.000). Our results show that eIF2α is largely cytoplasmically expressed in both the tumor and NNT collectives and is expressed in the UC in only 2 of 105 tumor cases (1.9%). Nuclear mean staining intensities of only 0.06 (IRS=0.40) were obtained in the tumor collective and 0.00 (IRS=0.00) in the NNT collective (p=0.157) (Table II, Figure 3, Figure 4).

Expression of eIF3a. The initiation factor showed cytoplasmic staining in both the tumor and the NNT collectives. Only two cases of the tumor collective (1.9%) showed expression of eIF3a in the nucleus. The nuclear staining intensity of eIF3a in the tumor and NT collectives was negligible, 0.03 (IRS=0.14) and 0.00 (IRS=0.00), respectively. With a cytoplasmic staining intensity averaging 1.57 (IRS=15.55), medium staining intensities (62 of 103 cases, 60.2%) accounted for the largest proportion in the

tumor collective. Weak staining was observed in 35 cases (34.0%). In only 5 cases (4.9%) there was no staining, and in one case (1.0%) a strong staining was detected. In healthy urothelial tissue, however, the average cytoplasmic staining intensity was only 1.21 (IRS=12.11). As in the tumor collective, most cases (41 out of 76 cases, 53.9%) showed rather moderately strong staining. Interestingly, no staining was detectable in 21 of 76 cases (27.6%). Fourteen cases (18.4%) showed weak cytoplasmic staining. A significantly higher cytoplasmic staining intensity of eIF3a was found in the UC (p=0.002) (Table II, Figure 3, Figure 4).

Expression of eIF3b. For the IHC expression analyses of eIF3b, 105 stainings of the tumor collective and 74 of the NNT collective were evaluated. Our results showed that this eIF was exclusively detected in the cytoplasm and in none of the cases it was expressed in the nucleus. eIF3b showed predominantly medium cytoplasmic staining in the UC (I=1.92, IRS=18.68). We observed strong positive staining in 25 of 105 cases (23.8%), medium staining in 51 (48.6%), and weak staining in 25 (23.8%). In four cases (3.8%), no staining was observed. In NNT tissue, on the other hand, no staining was obtained in 20 of totally 74 cases (27.0 %). Here, predominantly weak (27 cases, 36.5%) and moderately strong (25 cases, 33.8%) cytoplasmic stainings were detected. The average cytoplasmic staining intensity in the NT collective was only 1.07 (IRS=10.25). Using the Wilcoxon-test, on average, there was a significantly higher cytoplasmic expression of eIF3b in tumor tissues compared with that in NT tissues (p>0.000) (Table II, Figure 3, Figure 4).

Expression of eIF4b. Our results showed that eIF4b was mainly expressed in the cytoplasm and showed on average, weak to medium intensity of 1.56 (IRS=15.60) in the tumor collective. With 63 out of 105 tumor cases (60.0%), medium cytoplasmic staining (I=2) accounted for the largest proportion. In contrast, in the NNT collective the average staining intensity of 1.09 (IRS=10.76) was rather weak, and about half of all cases (35 of 75 cases, 46.7%) showed weak cytoplasmic staining. The Wilcoxon-test showed on average a significantly higher cytoplasmic staining of eIF4b in the UC (p=0.000). Nuclear average staining intensities only reached 0.10 (IRS=0.72) in the tumor collective and 0.04 (IRS=0.33) in the NT collective (p=0.125) (Table II, Figure 3, Figure 4).

Expression of eIF4e. For eIF4e, stainings from 104 patients of the tumor collective and 72 of the non-tumor collective were evaluable. In the tumor tissue, an average cytoplasmic staining of 1.66 (IRS=16.59) was observed. The NNT showed an intensity of 1.52 (IRS=15.16), whereas the cytoplasmic staining reactivity was similar. The initiation factor eIF4e was detectable in almost all cases of both collectives in the cytoplasm. In only one case of the tumor collective a weak nuclear staining was obtained. Using the Wilcoxon test, the comparison of the tumor and NNT collectives led to no significant differences for r cytoplasmic eIF4e expression (p=0.431) or for nuclear eIF4e expression (p=0.317) (Table II, Figure 3, Figure 4).

Expression of eIF4G. Our results showed an exclusively cytoplasmic expression of eIF4g in the tumor and NT collectives. In the CC, the initiation factor was not detected in any of the 73 NT and 105 tumor cases. With an average cytoplasmic staining of 2.27 (IRS=22.67) in the UC, eIF4g was significantly up-regulated (p=0.000) compared with the NNT collective (I=1.56 and IRS=15.36). Forty-four of 105 UC cases (41.9%) showed strong cytoplasmic staining, 48 cases (45.7%) showed moderate staining, and 10 cases (9.5%) weak staining. Three cases (2.9%) had no staining at all. Interestingly, in contrast, in the NNT collective, 20 of 73 cases (27.4%) did not show any cytoplasmic staining. Here, moderately strong (27 cases, 37.0%) and strong stainings (20 cases, 27.4%) accounted for the largest proportion (Table II, Figure 3, Figure 4).

Expression of eIF5a. For eIF5a, stainings from 105 patients of the tumor collective and 72 of the NNT collective were evaluated. In the tumor tissue, an average staining intensity of 1.19 (IRS=11.81) was found. In comparison, the NT tissue showed an average staining intensity of 1.48 (IRS=14.33). With an average intensity of 0.38 in the CC, the healthy urothelial tissue showed significantly higher staining intensities compared with the nucleus in urothelial carcinomas. Using the U-test, on average, there was significantly lower

→

Figure 4. *Urothelial carcinoma (UC) tissue without an immunohistochemical staining (I=0) (left) and non-neoplastic tissue (NNT) with a weak cytoplasmic intensity (I=1) (right) for eIF1 (1). Strongly stained NNT UC (I=3), mainly cytoplasmic (left). Healthy urothelial tissue with no staining (I=0) (right) for eIF1ay (2). Strongly stained UC (I=3), mainly cytoplasmic (left). Healthy urothelial tissue with no staining (I=0) (right) for eIF2α (3). Strongly stained UC (I=3), mainly cytoplasmic (left). Healthy urothelial tissue with no staining (I=0) (right) for eIF3a (4). Strongly stained UC (I=3), mainly cytoplasmic (left). Healthy urothelial tissue with no staining (I=0) (right) for eIF3b (5). Strongly stained UC (I=3), mainly cytoplasmic (left). Healthy urothelial tissue with no staining (I=0) (right) for eIF3c (6). Strongly stained UC (I=3), mainly cytoplasmic (left). Healthy urothelial tissue with no staining (I=0) (right) for eIF4e (7). Strongly stained UC (I=3), mainly cytoplasmic (left). Healthy urothelial tissue with no staining (I=0) (right) for eIF4g (8). Weakly stained UC tissue (left), mainly cytoplasmic. Healthy urothelial tissue with a moderate cytoplasmic and strong nuclear staining (right) for eIF5a (9). Strongly stained UC (I=3), mainly cytoplasmic (left). Healthy urothelial tissue with no staining (I=0) (right) for eIF5b (10). Strongly stained UC tissue (I=3), cytoplasmic and nuclear (left). No staining was obtained (I=0) in healthy tissue (right) for eIF6 (11). Strong cytoplasmic and nuclear (C) staining.*

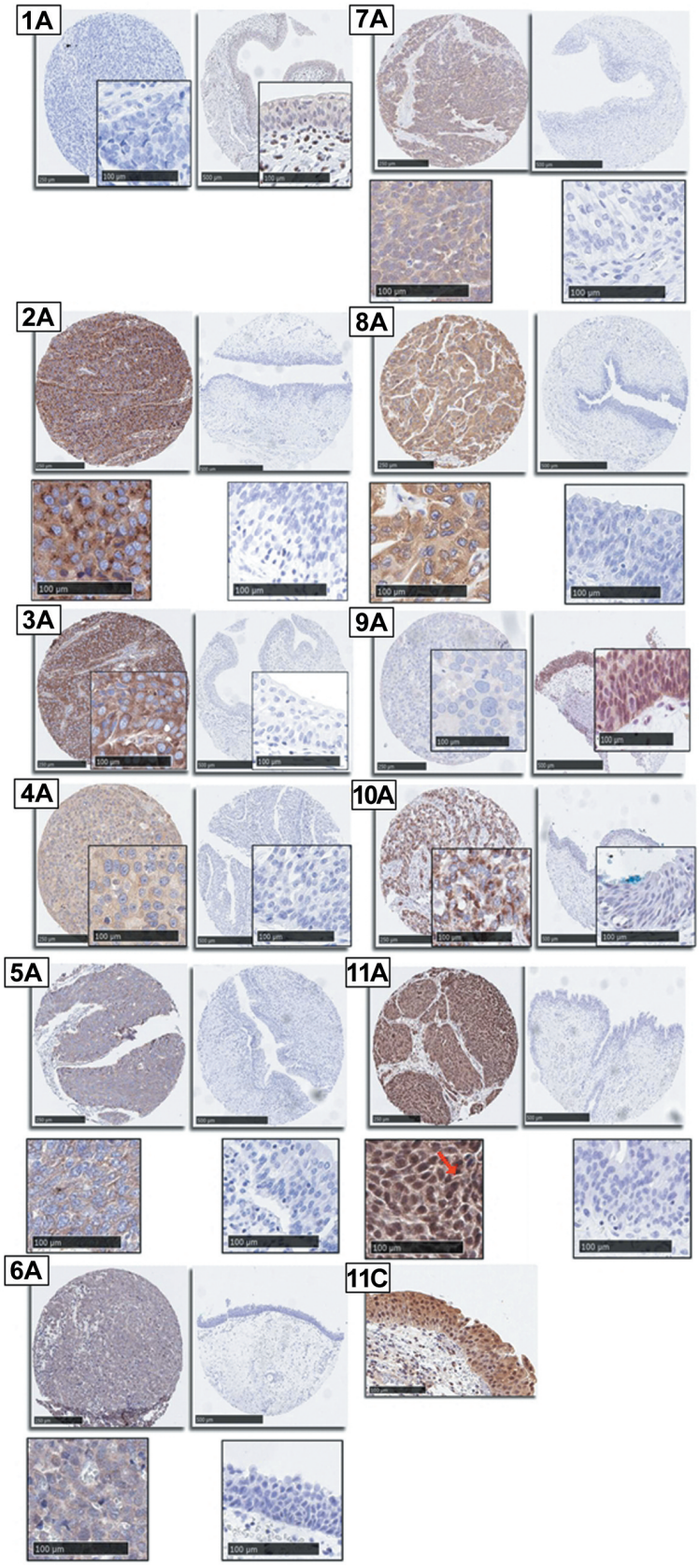
1A
7A
2A
8A
3A
9A
4A
10A
5A
11A
6A
11C

cytoplasmic expression of eIF5a in tumor tissue compared to NNT. Nuclear staining intensity was also significantly higher in healthy urothelial tissue (Table II, Figure 3, Figure 4).

Expression of eIF5b. EIF5b showed predominantly intermediate cytoplasmic staining intensity of 1.81 (IRS=17.22) in the UC. Fifteen of 105 cases (14.3%) showed strong, 59 (56.2%) showed moderately strong, and 27 (25.7%) showed weak stainings. In only 4 cases (3.8%) no staining was detected. In the cytoplasm of the NNT collective, the initiation factor was rather weakly to moderately expressed with an average staining intensity of 1.25 (IRS=11.05). Compared with the NNT collective, eIF5b was significantly up-regulated in the cytoplasm of the UC ($p>0.000$). Our results indicated that the initiation factor was mostly expressed in the cytoplasm in both the tumor and NNT collectives. In the nucleus, eIF5b was expressed in only 1 of 74 cases (1.4%). Nuclear average staining intensities of only 0.02 (IRS=0.08) in the tumor collective and 0.01 (IRS=0.01) in the NT collective ($p=0.655$) were found (Table II, Figure 3, Figure 4).

Expression of eIF6. EIF6 was expressed in the nucleus as well as in the cytoplasm of the Tumor and NNT collectives. With a cytoplasmic staining intensity averaging 2.56 (IRS=25.35), the initiation factor showed mostly strong staining (I=3) in 66 of 104 tumor samples (63.5%). Moderately strong staining intensities (I=2) were shown in 32 cases (30.8%). Four cases (3.8%) showed a weak cytoplasmic staining (I=1). In only two cases (1.9%) no staining was detected. In contrast, in healthy urothelial tissue, the average cytoplasmic color intensity was only 1.72 (IRS=16.64) and was rather moderate in most cases (28 of 74). Interestingly, in 18 out of 74 cases (24.3%) no staining was obtained. On average, the U-test revealed a significantly higher cytoplasmic staining intensity of eIF6 in the UC ($p>0.000$). Interestingly, the nuclear color intensity of eIF6 was significantly up-regulated in the NNT collective at 1.24 ($p=0.040$) (Table II, Figure 3, Figure 4).

Discussion

There is evidence that eIF1 may be involved in tumorigenesis (16, 17). Our results are consistent with those in the literature and show that eIF1 is significantly down-regulated in tumor tissue compared to control tissue. The average cytoplasmic color intensity in the tumor collective is only 0.23 (IRS=1.81). Surprisingly, the NNT collective has higher eIF1 expression with an average cytoplasmic staining intensity of 0.75 (IRS=6.80). Consistent with our results, Golob-Schwarzl *et al*. (17) using TMAs from pancreatic ductal adenocarcinomas, observed a significant down-regulation of certain eIFs in the cytoplasm of tumor tissues (n=174) compared to that in NNT tissues (n=10). We evaluated the expression behavior of eIF1 in the UC in terms of a potential tumor suppressor function. Interestingly, patients with low eIF1 expression had worse overall survival than those with high expression.

Unfortunately, there are hardly any studies dealing with the expression of eIF1AY in carcinomas. The two genes encoding the corresponding initiation factors eIF1AY and eIF1AX exhibit homology of approximately 86% (18). Our results showed that the initiation factor eIF1A in the UC is expressed with an average intensity of 2.76 (IRS=26.92) and is thus significantly up-regulated. In comparison, in the NNT collective, we observed a cytoplasmic staining intensity of only 1.16 (IRS=10.32). Furthermore, the initiation factor eIF1A (eIF1AX/eIF1aY) in the UC was mainly localized in the cytoplasm.

IF2 is a heterotrimeric protein whose gamma subunit is either GTP- or GDP-bound. In the GTP-bound state, eIF2 interacts with met-tRNAi to form the ternary complex (TC). This binds to the 40S subunit and forms the 43S-pre-initiation complex (PIC). The codon-anticodon interaction triggers GTP hydrolysis. The resulting eIF2-GDP dissociates from the mRNA and cannot participate in the reaction in this state. Only after eIF2b, a Guanosine triphosphate exchange factor (GEF), replaces GDP with GTP renewal of its participation is possible. However, recycling by eIF2b can be prevented by phosphorylation of the eIF2α subunit at the Ser-51 residue (19, 20). We demonstrated that eIF2α is significantly upregulated and mainly localized in the cytoplasm.

Spilka *et al*. (21) were the first to investigate the expression of eIF3a in UC. Consistent with our results, they showed that eIF3a is significantly up-regulated in the UC. In our patient collective, the average cytoplasmic staining intensity in the UC was 1.57 (IRS=15.55). In contrast, in the NNT collective, the cytoplasmic staining intensity was 1.21 (IRS=12.11). In squamous cell carcinomas of the oral cavity, it was shown that that eIF3a was up-regulated and mainly localized in the cytoplasm (22). We conclude from these observations that up-regulation of eIF3a may lead to increased translation and thus promotion of unhindered cell growth.

Interestingly, up-regulation of eIF3b has already been demonstrated in breast (23), colon (24), esophageal (25), prostate and urothelial carcinomas (26). This raises the fundamental question of the extent to which eIF3b is involved in carcinogenesis and its role in UC. Our results indicate that eIF3b shows a predominantly intermediate cytoplasmic staining in UC (I=1.92, IRS=18.68) and is significantly up-regulated compared to healthy urothelial tissue (I=1.07, IRS=10.25). We and also others evaluated the higher expression of eIF3b in tumor tissue in terms of a possible cause for the development of UC. Wang *et al*. (26), using *in vitro* experiments on the UC cell lines UMUC3 and LuL-2, showed that eIF3b silencing via siRNA transfection

slowed tumor growth and inhibited G1/S transition in the cell cycle. They hypothesized that by knocking down IF3b, the cell could remain in the G1 phase and thus tumor growth could be inhibited.

It was reported that the protooncogenic signaling pathways PI3-K/mTOR and Ras-MAPK, associated with proliferation and cell growth, regulate the activity of eIF4b by phosphorylation at the Ser-422 residue (27). This is consistent with its activation and higher translation rates and has been studied in numerous carcinomas (7). The question that arises is to what extent dysregulation of eIF4b may be involved in the development of UC and other tumor entities, and how this might be related to the mTOR pathway. We found significantly higher eIF4b expression in UC compared to NNT tissue. Showing cytoplasmic staining intensity of 1.56 on average (IRS=15.60), eIF4b is rather moderately expressed in UC. In contrast, in the NNT tissue, weak staining (I=1.09, IRS=10.76) accounted for the largest proportion. We evaluated these results as a potential cause for the development of UC. We hypothesize that up-regulation of eIF4b in UC leads to overstimulation of helicase activity of eIF4a, thus leading to uncontrolled cell proliferation and increased translation rates.

eIF4e, as part of the eIF4f complex, plays a key role in translation initiation and has been suggested by numerous studies as being primarily responsible for carcinogenesis. As a downstream target of the protooncogenic mTOR pathway, eIF4e is regulated by 4E-BP1 and -2 that dock to it. Positive growth stimuli lead to phosphorylation and consequently dissociation of 4E-BP from eIF4e with the help of the so-called mTOR kinases. The now activated eIF4e recognizes and binds to the 5' cap of the mRNA, leading to the formation of the eIF4f complex for translation to proceed (7, 28). In athymic mouse models intravesically implanted with UC-derived Ku-7-Luc cells, Chi *et al*. (29) investigated the dual inhibition of the mTOR downstream targets p70S6K and eIF4e.

Cap-dependent translation plays a critical role in the translation of protooncogenic proteins and is tightly regulated in the initiation phase, the rate-determining step of protein biosynthesis (30). In order for translation to proceed, the 5'-cap of the mRNA is recruited to the ribosome with the help of the eIF4f complex. The formation of eIF4f is strongly dependent on the interaction between eIF4g, the scaffold of the complex, and eIF4e, a cap-binding protein that binds the mRNA (31). The eIF4e/4g binding is competitively regulated by 4E-BPs that bind to eIF4e. After phosphorylation by mTOR kinases, the 4E-BPs dissociate from eIF4e and enable the eIF4e/4g interaction (32). Our results show that this initiation factor is significantly up-regulated in UC compared to the NNT collective. In the tumor collective, a mainly cytoplasmic staining was observed with an average staining intensity of 2.27 (IRS=22.67). In comparison, the staining intensity in the NNT collective averaged 1.56 (IRS=15.36). In both the tumor and NNT collectives, no nuclear staining was observed in any of the cases. The localization of the staining can be explained by the function of the initiation factor during translation in the cytoplasm.

In glioblastomas, it has been shown that eIF5a1 and its activation by modification appear to play a crucial role in carcinogenesis (33). The authors demonstrated a significant up-regulation of eIF5a1 and the hypusination enzymes DHS and DOHH in 173 glioblastoma samples. Inhibition of hypusination with N1-guanyl-1,7-diaminoheptane (GC7), a DHS inhibitor (34), resulted in a strong antiproliferative effect in glioblastoma cell lines. By *in vitro* knockdown of eIF5a1 and DHS using small hairpin RNA (shRNA), the authors were able to mimic the antiproliferative effects of GC7. These results suggest that hypusination may play an important role in carcinogenesis and may also be of interest in UC progression. Consistent with our results, there are studies showing that eIF5a1 may act not only as an oncogene but also as a tumor suppressor. In knock-out mouse models, it was shown that shRNA-mediated knockdown of eIF5a1 and the enzymes of hypusine synthesis, spermidine synthase, and DHS promoted the development of B-cell Non-Hodgkin Lymphoma *in vivo* (35). Our results in UC show decreased eIF5a1 expression in the tumor collective and suggest a tumor suppressor function that may be regulated by hypusine modification. We evaluated the up-regulation in healthy urothelial tissue in terms of a possible tumor suppressor function of eIF5a for the development of UC. Surprisingly, the initiation factor was found both in the cytoplasm and nucleus in 62 urothelial tissues, whereas in carcinoma tissue we observed almost exclusively cytoplasmic expression. It is reasonable to hypothesize that when eIF5a1 is decreased during UC carcinogenesis, nucleocytoplasmic export of protooncogenic mRNAs may occur. This conjecture is supported by studies that assume that eIF5a1 represents a shuttle protein whose export from the nucleus is facilitated by interactions with exportin-1 and exportin-4 (36, 37).

Dysregulation of all these mentioned functions of eIF5b could play a key role in carcinogenesis and result in aberrant protein expression. Our results show significant up-regulation of eIF5b in the cytoplasm in UC. The average cytoplasmic staining intensity of the tumor collective composed of 105 patients was 1.81 (IRS=17.22). In the NNT collective, which consisted of 74 patients, the cytoplasmic staining intensity was only 1.25 (11.05). Based on our results, we suggest that the GTPase function of this initiation factor may play a crucial role in the carcinogenesis of UC. Rapidly growing cancer cells have a huge energy demand to maintain their metabolic rate. Dysfunction and up-regulation of certain subfamilies of small regulatory GTPases, such as Arf and Ras, have been demonstrated in numerous cancers

(38). Up-regulation of the initiation factor eIF5b could accelerate the formation of the translational 80S ribosome and the transition from the initiation phase to the elongation phase. This could result in increased and uncontrolled translation, which may lead to translation of protooncogenic mRNA sequences.

The mammalian ribosome is composed of a small 40S and a large 60S subunit. The site of origin of ribosomes is the nucleus, which contains so-called ribosomal RNAs (rRNA) that serve as building blocks. EIF6 plays an important role during ribosome biogenesis and binds to the immature 60S subunit within the nucleus. A nucleo-cytoplasmic export of the immature ribosomes to the cytoplasm subsequently occurs, where eIF6 dissociates to allow the formation of the mature 80S ribosome in the final step of translation initiation (39, 40). Through its binding to the 60S subunit, eIF6 represents an important regulatory node and, as a so-called anti-association factor, prevents the premature assembly of the two parts (40, 41). Interestingly, our results show dysregulation of eIF6 in the UC. We found significantly higher eIF6 expression in UC compared to that in NT tissue. With a cytoplasmic staining intensity of 2.56 on average (IRS=25.35), eIF6 was strongly expressed in UC. In contrast, in healthy urothelial tissue, the average cytoplasmic staining intensity was only 1.72 (IRS=16.64) and was moderately expressed in most cases. We evaluated the up-regulation of eIF6 in the cytoplasm of the tumor collective in terms of increased translation and as a possible origin of UC. Dysregulation of eIF6 would allow the initiation factor to function as an anti-association factor and accelerate the premature assembly of the ribosome subunits to form the translatable 80S ribosome. Our results are supported by a study by Golob-Schwarzl *et al*. (40), in which the expression of eIF6 was investigated in gallbladder carcinomas (GBC). Using IHC analyses of TMAs consisting of 114 tissue samples, the authors observed significantly higher, cytoplasmic eIF6 expression in carcinomas compared to healthy control tissues. To support their findings, the authors also performed immunoblot analysis on cryotissues from 14 GBCs and 12 non-neoplastic altered gallbladders, which also revealed an up-regulation in the cytoplasm of GBCs. In the next step, the authors investigated the effect of siRNA-mediated knockdown of eIF6 in GBC cell lines. In the MzChA-2 and TFK-1 cell lines, there was significantly reduced cell proliferation and increased apoptosis rates.

Conclusion

Our findings strongly support a dysregulation of various eIFs in UC. Whereas eIF1aY, eIF2α, eIF3a, eIF3b, eIF4b, eIF4g, eIF5b, and eIF6 were up-regulated in the cytoplasm of UC, eIF1 and eIF5 were down-regulated, and eIF5 and eIF6 were decreasingly expressed in the nucleus of the UC cells. Data on the expression of eIFs in UC are very limited. The aim of our work was to supplement this and to analyze the expression behavior of additional eIFs in UC. For this purpose, FFPE tissue samples from 107 patients with UC were embedded in TMA blocks and subsequently examined using IHC. The healthy urothelial tissue of the patient collective was used as comparative tissue.

The main results of the present work can be summarized as follows: eIFs are dysregulated in UC: eIF1aY, 2α, 3a, 3b, 4b, 4g, 5b, and eIF6 are up-regulated in the cytoplasm of UC cells, eIF1 and eIF5a are down-regulated in the cytoplasm of the UC, eIF5a and eIF6 are down-regulated in the cytoplasm of the UC.

Eukaryotic translation and the associated molecular biological processes have gained increasing attention in cancer research. The initiation of translation is tightly regulated, and this is enabled by the interplay of eIFs. There is ample evidence in the literature that dysregulation of eIFs may contribute to uninhibited growth and consequently to tumorigenesis (7). Rapidly proliferating tumor cells require increased protein biosynthesis and have increased energy requirements. This suggests that protein synthesis rates play an essential role in the control of cell growth (8). Dysregulation of eIFs in the first step of protein biosynthesis, the so-called translation initiation, may play a key role in this process and turn eIFs into therapeutic targets.

Conflicts of Interest

The Authors declare no conflicts of interest in relation to this study.

Authors' Contributions

Conceptualization, J.H. and J.L.; methodology, J.H., J.L., N.N.; software, J.L.; validation; formal analysis, J.L.; investigation, JL, N.S., N.Sc., T.K., J.H., P.C., N.N.; resources, J.H., B.J., M.S.; writing—original draft preparation, J.L.,; writing—review and editing, J.L., C.S., N.S., N.Sc., T.K., J.H., N.N.; visualization: C.S.; supervision, J.H.; project administration, J.L.; funding acquisition, J.H. All Authors have read and agreed to the published version of the manuscript.

References

1 S3-Leitlinie Harnblasenkarzinom. 400(2020). Available at: https://www.leitlinienprogramm-onkologie.de/fileadmin/user_upload/Downloads/Leitlinien/Blasenkarzinom/Version_2.0/LL_Harnblasenkarzinom_Langversion_2.0.pdf [Last accessed on January 23, 2023]

2 Antoni S, Ferlay J, Soerjomataram I, Znaor A, Jemal A and Bray F: Bladder cancer incidence and mortality: a global overview and recent trends. Eur Urol *71(1)*: 96-108, 2017. PMID: 27370177. DOI: 10.1016/j.eururo.2016.06.010

3 Dobruch J, Daneshmand S, Fisch M, Lotan Y, Noon AP, Resnick MJ, Shariat SF, Zlotta AR and Boorjian SA: Gender and bladder cancer: a collaborative review of etiology, biology, and outcomes. Eur Urol *69(2)*: 300-310, 2016. PMID: 26346676. DOI: 10.1016/j.eururo.2015.08.037

4 Cumberbatch MGK, Jubber I, Black PC, Esperto F, Figueroa JD, Kamat AM, Kiemeney L, Lotan Y, Pang K, Silverman DT, Znaor A and Catto JWF: Epidemiology of bladder cancer: a systematic review and contemporary update of risk factors in 2018. Eur Urol *74(6)*: 784-795, 2018. PMID: 30268659. DOI: 10.1016/j.eururo.2018.09.001

5 Letašiová S, Medve'ová A, Šovčíková A, Dušinská M, Volkovová K, Mosoiu C and Bartonová A: Bladder cancer, a review of the environmental risk factors. Environ Health *11(Suppl 1)*: S11, 2012. PMID: 22759493. DOI: 10.1186/1476-069X-11-S1-S11

6 Pestova TV, Hellen CU and Shatsky IN: Canonical eukaryotic initiation factors determine initiation of translation by internal ribosomal entry. Mol Cell Biol *16(12)*: 6859-6869, 1996. PMID: 8943341. DOI: 10.1128/MCB.16.12.6859

7 Spilka R, Ernst C, Mehta AK and Haybaeck J: Eukaryotic translation initiation factors in cancer development and progression. Cancer Lett *340(1)*: 9-21, 2013. PMID: 23830805. DOI: 10.1016/j.canlet.2013.06.019

8 Silvera D, Formenti SC and Schneider RJ: Translational control in cancer. Nat Rev Cancer *10(4)*: 254-266, 2010. PMID: 20332778. DOI: 10.1038/nrc2824

9 Sonenberg N and Hinnebusch AG: Regulation of translation initiation in eukaryotes: mechanisms and biological targets. Cell *136(4)*: 731-745, 2009. PMID: 19239892. DOI: 10.1016/j.cell.2009.01.042

10 Jaiswal PK, Koul S, Palanisamy N and Koul HK: Eukaryotic translation initiation factor 4 Gamma 1 (EIF4G1): a target for cancer therapeutic intervention? Cancer Cell Int *19*: 224, 2019. PMID: 31496918. DOI: 10.1186/s12935-019-0947-2

11 Yin JY, Dong Z, Liu ZQ and Zhang JT: Translational control gone awry: a new mechanism of tumorigenesis and novel targets of cancer treatments. Biosci Rep *31(1)*: 1-15, 2011. PMID: 20964625. DOI: 10.1042/BSR20100077

12 Lorsch JR and Dever TE: Molecular view of 43 S complex formation and start site selection in eukaryotic translation initiation. J Biol Chem *285(28)*: 21203-21207, 2010. PMID: 20444698. DOI: 10.1074/jbc.R110.119743

13 Jackson RJ, Hellen CU and Pestova TV: The mechanism of eukaryotic translation initiation and principles of its regulation. Nat Rev Mol Cell Biol *11(2)*: 113-127, 2010. PMID: 20094052. DOI: 10.1038/nrm2838

14 Algire MA and Lorsch JR: Where to begin? The mechanism of translation initiation codon selection in eukaryotes. Curr Opin Chem Biol *10(5)*: 480-486, 2006. PMID: 16935023. DOI: 10.1016/j.cbpa.2006.08.010

15 Kapp LD and Lorsch JR: The molecular mechanics of eukaryotic translation. Annu Rev Biochem *73*: 657-704, 2004. PMID: 15189156. DOI: 10.1146/annurev.biochem.73.030403.080419

16 Lian Z, Pan J, Liu J, Zhang S, Zhu M, Arbuthnot P, Kew M and Feitelson MA: The translation initiation factor, hu-Sui1 may be a target of hepatitis B X antigen in hepatocarcinogenesis. Oncogene *18(9)*: 1677-1687, 1999. PMID: 10208429. DOI: 10.1038/sj.onc.1202470

17 Golob-Schwarzl N, Puchas P, Gogg-Kamerer M, Weichert W, Göppert B and Haybaeck J: New pancreatic cancer biomarkers eIF1, eIF2D, eIF3C and eIF6 play a major role in translational control in ductal adenocarcinoma. Anticancer Res *40(6)*: 3109-3118, 2020. PMID: 32487605. DOI: 10.21873/anticanres.14292

18 Yarahmadi E, Borjian Boroujeni P, Totonchi M and Gourabi H: Genotyping of the EIF1AY gene in Iranian patients with non-obstructive azoospermia. Curr Urol *13(1)*: 46-50, 2019. PMID: 31579209. DOI: 10.1159/000499295

19 Maida I, Zanna P, Guida S, Ferretta A, Cocco T, Palese LL, Londei P, Benelli D, Azzariti A, Tommasi S, Guida M, Pellacani G and Guida G: Translational control mechanisms in cutaneous malignant melanoma: the role of eIF2α. J Transl Med *17(1)*: 20, 2019. PMID: 30634982. DOI: 10.1186/s12967-019-1772-z

20 Sesma A, Castresana C and Castellano MM: Regulation of translation by TOR, eIF4E and eIF2α in plants: current knowledge, challenges and future perspectives. Front Plant Sci *8*: 644, 2017. PMID: 28491073. DOI: 10.3389/fpls.2017.00644

21 Spilka R, Ernst C, Bergler H, Rainer J, Flechsig S, Vogetseder A, Lederer E, Benesch M, Brunner A, Geley S, Eger A, Bachmann F, Doppler W, Obrist P and Haybaeck J: eIF3a is over-expressed in urinary bladder cancer and influences its phenotype independent of translation initiation. Cell Oncol (Dordr) *37(4)*: 253-267, 2014. PMID: 25070653. DOI: 10.1007/s13402-014-0181-9

22 Spilka R, Laimer K, Bachmann F, Spizzo G, Vogetseder A, Wieser M, Müller H, Haybaeck J and Obrist P: Overexpression of eIF3a in squamous cell carcinoma of the oral cavity and its putative relation to chemotherapy response. J Oncol *2012*: 901956, 2012. PMID: 22619676. DOI: 10.1155/2012/901956

23 Hershey JW: The role of eIF3 and its individual subunits in cancer. Biochim Biophys Acta *1849(7)*: 792-800, 2015. PMID: 25450521. DOI: 10.1016/j.bbagrm.2014.10.005

24 Wang Z, Chen J, Sun J, Cui Z and Wu H: RNA interference-mediated silencing of eukaryotic translation initiation factor 3, subunit B (EIF3B) gene expression inhibits proliferation of colon cancer cells. World J Surg Oncol *10*: 119, 2012. PMID: 22734884. DOI: 10.1186/1477-7819-10-119

25 Xu F, Xu CZ, Gu J, Liu X, Liu R, Huang E, Yuan Y, Zhao G, Jiang J, Xu C, Chu Y, Lu C and Ge D: Eukaryotic translation initiation factor 3B accelerates the progression of esophageal squamous cell carcinoma by activating β-catenin signaling pathway. Oncotarget *7(28)*: 43401-43411, 2016. PMID: 27270324. DOI: 10.18632/oncotarget.9726

26 Wang H, Ru Y, Sanchez-Carbayo M, Wang X, Kieft JS and Theodorescu D: Translation initiation factor eIF3b expression in human cancer and its role in tumor growth and lung colonization. Clin Cancer Res *19(11)*: 2850-2860, 2013. PMID: 23575475. DOI: 10.1158/1078-0432.CCR-12-3084

27 Shahbazian D, Parsyan A, Petroulakis E, Hershey J and Sonenberg N: eIF4B controls survival and proliferation and is regulated by proto-oncogenic signaling pathways. Cell Cycle *9(20)*: 4106-4109, 2010. PMID: 20948310. DOI: 10.4161/cc.9.20.13630

28 Chen YT, Tsai HP, Wu CC, Wang JY and Chai CY: Eukaryotic translation initiation factor 4E (eIF-4E) expressions are associated with poor prognosis in colorectal adenocarcinoma. Pathol Res Pract *213(5)*: 490-495, 2017. PMID: 28242042. DOI: 10.1016/j.prp.2017.02.004

29 Chi BH, Kim SJ, Seo HK, Seo HH, Lee SJ, Kwon JK, Lee TJ and Chang IH: P70S6K and Elf4E dual inhibition is essential to control bladder tumor growth and progression in orthotopic mouse non-muscle invasive bladder tumor model. J Korean Med Sci *30(3)*: 308-316, 2015. PMID: 25729255. DOI: 10.3346/jkms.2015.30.3.308

30 Oblinger JL, Burns SS, Akhmametyeva EM, Huang J, Pan L, Ren Y, Shen R, Miles-Markley B, Moberly AC, Kinghorn AD, Welling DB and Chang LS: Components of the eIF4F complex are potential therapeutic targets for malignant peripheral nerve

sheath tumors and vestibular schwannomas. Neuro Oncol *18(9)*: 1265-1277, 2016. PMID: 26951381. DOI: 10.1093/neuonc/now032

31 Dobrikov M, Dobrikova E, Shveygert M and Gromeier M: Phosphorylation of eukaryotic translation initiation factor 4G1 (eIF4G1) by protein kinase C{alpha} regulates eIF4G1 binding to Mnk1. Mol Cell Biol *31(14)*: 2947-2959, 2011. PMID: 21576361. DOI: 10.1128/MCB.05589-11

32 Li L, Luo Q, Xie Z, Li G, Mao C, Liu Y, Wen X, Yin N, Cao J, Wang J, Li L, Yu J, Wang F and Yi P: Characterization of the expression of the RNA binding protein eIF4G1 and its clinicopathological correlation with serous ovarian cancer. PLoS One *11(9)*: e0163447, 2016. PMID: 27668427. DOI: 10.1371/journal.pone.0163447

33 Preukschas M, Hagel C, Schulte A, Weber K, Lamszus K, Sievert H, Pällmann N, Bokemeyer C, Hauber J, Braig M and Balabanov S: Expression of eukaryotic initiation factor 5A and hypusine forming enzymes in glioblastoma patient samples: implications for new targeted therapies. PLoS One *7(8)*: e43468, 2012. PMID: 22927971. DOI: 10.1371/journal.pone.0043468

34 Turpaev KT: Translation factor eIF5A, modification with hypusine and role in regulation of gene expression. eIF5A as a target for pharmacological interventions. Biochemistry (Mosc) *83(8)*: 863-873, 2018. PMID: 30208826. DOI: 10.1134/S0006297918080011

35 A tumour suppressor network relying on the polyamine–hypusine axis | Nature. Available at: https://www.nature.com/articles/nature11126 [Last accessed on July 17, 2022]

36 Wu GQ, Xu YM and Lau ATY: Recent insights into eukaryotic translation initiation factors 5A1 and 5A2 and their roles in human health and disease. Cancer Cell Int *20*: 142, 2020. PMID: 32368188. DOI: 10.1186/s12935-020-01226-7

37 Lee SB, Park JH, Kaevel J, Sramkova M, Weigert R and Park MH: The effect of hypusine modification on the intracellular localization of eIF5A. Biochem Biophys Res Commun *383(4)*: 497-502, 2009. PMID: 19379712. DOI: 10.1016/j.bbrc.2009.04.049

38 Prieto-Dominguez N, Parnell C and Teng Y: Drugging the small GTPase pathways in cancer treatment: promises and challenges. Cells *8(3)*: 255, 2019. PMID: 30884855. DOI: 10.3390/cells8030255

39 Gantenbein N, Bernhart E, Anders I, Golob-Schwarzl N, Krassnig S, Wodlej C, Brcic L, Lindenmann J, Fink-Neuboeck N, Gollowitsch F, Stacher-Priehse E, Asslaber M, Gogg-Kamerer M, Rolff J, Hoffmann J, Silvestri A, Regenbrecht C, Reinhard C, Pehserl AM, Pichler M, Sokolova O, Naumann M, Mitterer V, Pertschy B, Bergler H, Popper H, Sattler W and Haybaeck J: Influence of eukaryotic translation initiation factor 6 on non-small cell lung cancer development and progression. Eur J Cancer *101*: 165-180, 2018. PMID: 30077122. DOI: 10.1016/j.ejca.2018.07.001

40 Golob-Schwarzl N, Wodlej C, Kleinegger F, Gogg-Kamerer M, Birkl-Toeglhofer AM, Petzold J, Aigelsreiter A, Thalhammer M, Park YN and Haybaeck J: Eukaryotic translation initiation factor 6 overexpression plays a major role in the translational control of gallbladder cancer. J Cancer Res Clin Oncol *145(11)*: 2699-2711, 2019. PMID: 31586263. DOI: 10.1007/s00432-019-03030-x

41 Brina D, Miluzio A, Ricciardi S and Biffo S: eIF6 anti-association activity is required for ribosome biogenesis, translational control and tumor progression. Biochim Biophys Acta *1849(7)*: 830-835, 2015. PMID: 25252159. DOI: 10.1016/j.bbagrm.2014.09.010

Received January 12, 2023
Revised January 25, 2023
Accepted February 1, 2023